Journal of Engineering, Science and Technology
ISSN: 2714-2396, Volume 9 Issue 1

PERFORMANCE ANALYSIS OF ENVIRONMENTAL AND ELECTRICAL DERATING FACTORS IN RESIDENTIAL PHOTOVOLTAIC SYSTEMS

E. S. Chukwuebuka [1], I. F. Udebunu[2*], C. E. Obasi [3*]

[1, 2, 3] Enugu State University of Science and Technology

Corresponding email: Edeanics@gmail.com

Received: 14 May 2026 **Accepted**: Date 30 May 2026 **Published**: 16 June 2026

Abstract. This study was motivated by recurring complaints from photovoltaic (PV) system users regarding a noticeable decline in power output after extended periods of operation. It presents a performance analysis of environmental derating and electrical derating factors influencing the efficiency and reliability of PV systems. The study evaluates the influence of ambient temperature, dust, and parallel-string configuration on voltage drop and resistive power losses in DC cabling networks in tropical climate. Results show that PV module performance decreases with increasing cell temperature and prolonged dust accumulation: as the cell temperature increased from 25°C to 75°C, the normalized power output declined by approximately 20% across all irradiance levels, with power at 1000 W/m² decreasing from 1.00 to 0.80. Similar trends were observed at irradiance levels of 800 W/m², 600 W/m², and 400 W/m², indicating a nearly linear reduction in power output with temperature rise. In addition to these, the effect of dust accumulation on energy yield was significant, it resulted in a relative daily energy output steady decrease from 100% for a clean panel to 76% after eight weeks without cleaning, representing a total energy loss of 24%. Dust deposition shows an average energy reduction of approximately 3% per week. Overall, the findings demonstrate that both elevated operating temperatures and dust accumulation adversely affect PV system performance, with dust accumulation exhibiting a slightly greater impact on energy yield than temperature under the illustrated conditions.

Keywords: Photovoltaic systems, environmental derating, electrical derating, DC cabling networks, tropical climate.

1. Introduction

Residential PV systems have transitioned from niche applications to essential energy infrastructure in response to the global shift toward renewables and escalating electricity demand [1], [2], [3]. However, a persistent "performance gap" exists between manufacturer-rated standard test conditions (STC) and field-delivered energy, particularly in tropical regions like South-South Nigeria. In these locales, the synergy of elevated ambient temperatures, high humidity, and seasonal aerosol deposition (Harmattan dust) creates a complex derating environment that significantly compromises energy yield and system longevity [4], [5]. While existing research has documented individual stressors such as the thermal coefficients of modules or the impact of soiling, there remains a critical lack of integrated analysis that simultaneously correlates regional atmospheric variability with electrical balance-of-system (BOS) losses. Current literature often treats environmental derating and technical losses (e.g., cable resistive losses and inverter mismatch) as separate variables. This fragmentation leads to "oversimplified" design models that fail to account for how tropical humidity and temperature cycles accelerate the degradation of both the PV cells and the DC distribution infrastructure [6]. Furthermore, most standardized PV performance models are derived from temperate climates, leaving a methodological void in predicting the performance of residential systems in the high-humidity, low-wind-speed conditions characteristic of the South-South Nigerian coast. This study addresses this gap by evaluating PV performance under such conditions from parametric data obtained from related work.

1.1 Related work

The operational performance of photovoltaic (PV) systems is not merely a function of solar irradiance but a complex interplay of environmental derating factors. While early literature often treated these variables in isolation, this study reveals a more synergistic, and damaging, reality. As shown in Table 1 below, there is a clear consensus on the severity of environmental impact, yet researchers differ on which specific variable dictates the highest performance loss.

Table 1: Comparative Impact of Environmental Stressors

Study	Primary Variable	Peak Reported Loss	Methodology	Key Finding
Sepúlveda-Oviedo [7]	Multi-factor (Deposition/Weather)	60–70%	Meta-analysis (175 papers)	Emphasizes standardized AI monitoring for multi-level degradation.
Dawood et al. [8]	Humidity & Temperature	~30% (Humidity alone)	Experimental/Empirical	Identified 55°C as a thermal tipping point for peak current before efficiency drops.

A critical contradiction emerges when comparing the role of wind: Dawood et al. [8] frame wind as a beneficial cooling mechanism that bolsters efficiency, whereas broader longitudinal studies cited by Sepúlveda-Oviedo [7] suggest that wind also acts as a transport agent for atmospheric deposition (soiling), which can lead to long-term abrasive degradation. This suggests that the "net benefit" of wind is likely region-specific, depending on whether the site is characterized by high ambient heat (benefiting from cooling) or high particulate matter (suffering from soiling). Furthermore, while Dawood provides specific empirical thresholds (e.g., the 30% humidity loss), Sepúlveda-Oviedo argues that these snapshots are insufficient without standardized metrics like the Cleanness Index, highlighting a gap between raw experimental data and actionable maintenance modelling.

The degradation of PV does not stop at cell surface; it extends into the balance-of-system (BOS) components, specifically DC cabling. There is a direct, often overlooked theoretical link between environmental heat and cable efficiency: as ambient temperatures rise, a factor

Dawood [8] identified as a primary stressor, the internal resistance of DC cabling increases, compounding the energy yield losses. Research by [9], [10] establishes that DC cabling is the "bottleneck" of energy delivery. However, a critical tension exists in the literature regarding "optimal" sizing:

1. The Performance Argument [11]: Undersized cables lead to resistive losses that erode the system's lifetime climate benefits.
2. The Economic Argument [12]: Excessive oversizing yields diminishing returns, where the marginal increase in kWh does not justify the capital expenditure (CAPEX) of copper.

A significant finding in recent studies [13], [14], [15] introduces a third variable: UV Ageing. While standard electrical engineering models focus on resistive losses due to diameter, these studies show that insulation resistance drops *exponentially* when exposed to the same UV and wind factors that affect the panels. This suggests that cable sizing in tropical or semi-arid regions cannot be calculated using standard temperature coefficients alone; it must account for the accelerated "dielectric fatigue" caused by the environment.

The novelty of this work lies in its integrated approach: rather than analysing stressors in isolation, this study develops a site-specific performance framework that quantifies the combined impact of environmental variables (temperature, humidity, and dust) alongside electrical derating factors. Consequently, the methodology of this study moves beyond simple "clear sky" calculations. It synthesizes the environmental thresholds identified by Dawood with the cable degradation models of [15], and adopts a centralized inverter placement strategy [14].

2. Material And Method

2.1 Research Design

This study adopted a simulation-based research design to evaluate the effects of temperature and dust accumulation on PV system performance. It relied on secondary data and established photovoltaic performance models reported in peer-reviewed journal articles and technical publications. Mathematical relationships describing the influence of temperature and dust deposition on PV output were implemented in a simulation environment to investigate their impact on power generation and energy yield.

2.2 Data Collection and Sources

The data used in this study were obtained from published literature on photovoltaic system performance. Relevant journals, conference papers, and technical reports were reviewed to identify commonly accepted PV operating parameters such as irradiance levels, temperature coefficients, and dust-induced degradation rates. Information extracted from these sources was used to develop the simulation model and define the operating conditions for the study.

2.3 Mathematical Modelling

The performance of the PV system under varying environmental conditions was represented using mathematical models derived from established photovoltaic theory. The normalized power output was calculated for different irradiance levels across the specified temperature range. For dust accumulation analysis, the relative energy yield of the PV system was modelled as a function of the duration of dust deposition on the panel surface. The model assumed a progressive reduction in energy production with increasing dust accumulation, consistent with findings reported in previous studies.

2.4 Simulation Procedure

The developed mathematical models were implemented using simulation software to evaluate PV performance under different operating conditions. The simulation was conducted in two stages:

1. Temperature Effect Analysis: The PV model was simulated at irradiance levels of 400 W/m², 600 W/m², 800 W/m², and 1000 W/m². For each irradiance level, cell temperature was varied from 25°C to 75°C in increments of 10°C. The corresponding normalized power output was calculated and recorded.
2. Dust Accumulation Analysis: The effect of dust accumulation was simulated over an eight-week period. The relative daily energy yield was determined for each week without panel cleaning. The reduction in energy production due to dust deposition was calculated and compared with the clean-panel condition.

2.5 Data Analysis

The simulation outputs were analysed using descriptive statistical techniques and graphical analysis. Performance trends were evaluated by observing changes in normalized power output and relative energy yield under varying temperature and dust conditions.

The following performance indicators were determined:

1. Maximum and minimum power output.
2. Percentage power reduction due to temperature increase.
3. Relative daily energy yield.
4. Percentage energy loss due to dust accumulation.
5. Overall performance trends under different environmental conditions.

The generated datasets were plotted using graphical tools to illustrate the relationships between temperature and power output, as well as dust accumulation and energy yield.

2.6 Validation of Results

To ensure the reliability of the simulation results, the generated performance trends were compared with observations from field installations and findings reported in previous photovoltaic performance studies. Several clients had reported a gradual reduction in photovoltaic system output over time, particularly during periods of prolonged exposure to high temperatures and infrequent panel cleaning. The simulation results exhibited similar behaviour, showing a decrease in power output with increasing cell temperature and a decline in energy yield as dust accumulation increased. These trends were also consistent with established findings in the literature, thereby providing confidence that the developed model reasonably represents the operating conditions experienced in practical PV installations.

2.7 Study Location and Simulation Environment

The geographical focus of this study is Enugu, Nigeria, characterized by a high-humidity tropical climate.

1. Environmental Data Synthesis: Rather than utilizing a single-year snapshot, the meteorological inputs for this study—including hourly solar irradiance, ambient temperature, and relative humidity were synthesized from a comprehensive meta-analysis of longitudinal climatic studies specific to the South-South Nigerian region. This approach ensures that the simulation parameters reflect the multi-year mean values for aerosol optical depth and thermal variability characteristic of the region, providing a more robust baseline for performance prediction than a single-site annual data point.
2. Simulation Tool: The system performance and cable voltage drops were modelled using (Python) to simulate real-world operating conditions against manufacturer Standard Test Conditions (STC).

2.8 Mathematical Modelling of Environmental Derating

To move beyond descriptive observations, the study utilizes the following mathematical models to quantify performance degradation.

2.8.1 Thermal and Irradiance Modelling

Equation (1) is actual power output P_{out} of a PV module, calculated by accounting for the temperature-dependent voltage drop. It is a derived equation [13], [16]:

$$P_{out} = G_{eff} * A * \eta_{mod} * [1 - \beta(T_{cell} - T_{ref})] \quad (1)$$

G_{eff}: Effective solar irradiance reaching the cell after accounting for dust/shading (W/m^2)
A: Total Surface Area of the PV array (m^2)
η_{mod}: Nominal module efficiency at STC
β: Temperature coefficient of power (typically -0.35 to -0.45%/^{o}C)
T_{cell}: Operating cell temperature, and T_{ref} is the reference temperature (25^{o}C)
The operating cell temperature (T_{cell}) is further modelled to include the cooling effect of wind and the insulating effect of humidity as seen in equation (2) [5]:

$$T_{cell} = T_{amb} + \left(\frac{NOCT-20}{800}\right) * G_{eff} \quad (2)$$

where NOCT is the Nominal Operating Cell Temperature provided by the manufacturer.

2.8.2 Environmental Stressor Coefficients (Humidity and Dust)

This study introduces a Cleanness Index (CI) and Humidity Derating Factor (f_{hum}) to adjust G_{eff} variable. Unlike generic models, we quantify the current reduction caused by water vapor scattering, particularly significant in Nigerian costal belt.

2.9 DC Cabling and Resistive Loss Analysis

A core novelty of this methodology is the treatment of DC cabling as a critical design variable. The electrical losses are governed by conductor resistance adjusted for the tropical thermal profile.

2.9.1 Resistance and Voltage Drop Equations

The resistance (R_0) of the DC cable is determined by equation (3) from Ohm's law:

$$R_0 = \rho \frac{L}{A} \quad (3)$$

ρ: Resistivity of the conductor material (Copper = $1.72x10^{-8}\Omega m$). L = Total length of the cable (m), A_{cond}: Cross-sectional area of the conductor (mm^2)
The voltage drop (∇V) for the DC string, accounting for the round-trip path from the array to the inverter, is expressed equation (4) [16]:

$$\nabla V = \frac{2*I*L*\rho}{A} \quad (4)$$

I: Operating current at Maximum Power Point (MPP)
The factor of 2 accounts for the total circuit length (positive and negative runs).

2.9.2 Impact on Inverter MPPT Efficiency

The study simulates how excessive ∇V (greater than the 2% industry threshold) shifts the operating point of the inverter. By calculating the Percentage Voltage Drop ($V_{drop\%}$) as given in equation (5):

$$V_{drop\%} = \left(\frac{\nabla V}{V_{mp}}\right) * 100 \quad (5)$$

V_{mp}: is the module voltage at maximum power used to evaluate whether environmental heat increases (equation (1)) enough to force the inverter outside its optimum MPPT window, thereby inducing secondary efficiency losses.

2.10 Simulation Parameters and Input Data

The following parameters (Table 2) define the "Base Case" for the residential layouts analysed in this study:

Table 2: *Simulation Parameters*

Parameter	Value	Units
PV Array Capacity	[e.g., 5.0]	kWp
Cable Material	Annealed Copper	-
Avg. Ambient Temp ()	[e.g., 32]	^{0}C
Relative Humidity (RH)	[e.g., 75-85]	%
Design Voltage Drop Target	< 2.0	%

2.11 Simulation Case Study: Numerical Validation

The computational model developed in Python is validated by establishing a representative residential PV case study.

2.11.1 Base Case Parameters

The simulation utilizes a standard 5 kWp residential array configuration. The input parameters, derived from typical installation practices in Nigeria, are summarized below:

1. System Power (P): 5 kw
2. Operating Voltage (V_{dc}): 250 V
3. One-way cable length (L): 30m (Total path $2L = 60m$)
4. Conductor Area (A): $6mm^2$(copper)
5. Resistivity (ρ): $1.72 * \ 10^{-8}\Omega m$

2.11.2 Stepwise Calculation and Theoretical Validation

The Python model executes the simulation following the standard resistive logic. To ensure accuracy, the model results were validated against the following manual derivation:

1. Operating Current (I): $I = \frac{P}{V_{dc}} = \frac{5000}{250} = 20A$
2. Round trip Resistance (R_{loop}): $R = \ \rho \frac{2L}{A} = 1.72 * 10^{-8} * \frac{60}{6*10^{-6}} = 0.172\Omega$
3. Voltage Drop (ΔV): $\Delta V = I * R = 20 * 0.172 = 3.44V$
4. Percentage Voltage Drop (V%)

2.12 Model Validation against International Standards

The Python model results (1.376%) were benchmarked against the IEC 60364-7-712 and BS 7671 standards, which recommend a maximum DC voltage drop of 3% (ideal) to 1% (high efficiency).

1. Standard Comparison: The simulation identifies that while a 6 mm² cable satisfies the 3% regulatory limit under STC, it approaches the marginal limit for high-efficiency design (target < 1.5%) when environmental heat is introduced.
2. Validation of Python Script: The convergence between the manual theoretical calculation and the Python output (yielding a 0% error margin under STC) validates the script's core algorithm before it is applied to the variable thermal data obtained from regional journals.

2.13 Thermal Correction and Real-World Reliability

Equation (6) gives an idealized resistance correction using the copper temperature coefficient (α = 0.00393) to enhance the model's fidelity for the South-South Nigerian context [16].

$$R_T = R_{ref}[1 + \alpha(T_{cable} - T_{ref}) \quad (6)$$

The resulting voltage drop in equation (5) is then recalculated as to include this ideation.

The iteration of these equations across the temperature ranges synthesized from literature enables the model to identify the "Critical Thermal Threshold" point at which standard-sized cables fail to meet the 2% efficiency requirement due to ambient heat alone.

2.14 PV System Topology and Cabling Architecture

The configuration of a PV array, whether series, parallel, or series-parallel, dictates the cumulative cable length and the resulting ohmic power losses. In this study, the inverter's nominal rating and MPPT voltage window determine the string length, while the total power requirement defines the number of parallel strings.

Equation (7) is derived for design current (I_{des}) when selecting conductor cross-sectional area.

$$I_{des} = \frac{I_{sc}*1.56}{0.58} \quad (7)$$

I_{sc}: Short-circuit current of the module at STC

1.58: A combined safety factor accounting for continuous load and irradiance enhancement (1.25*1.25)

0.58: A temperature derating factor specific to high-ambient tropical environments.

For an array consisting of multiple parallel strings (N_s), the total array current (I_{array}) is:

$$I_{array} = I_{des} * N_s$$

2.8.1 Component-Based Cable Length Modelling

Equation (8) is a derived equation that quantifies the resistive path of the total cable length (L_{total}) by modelling it as the sum of three distinct segments.

1. Module-to-Module (L_{mod}): The series interconnection within a string.
   $$L_{mod} = (L_{mod} + s) * k \quad (8)$$
   (L_{mod} is module length, *s* is spacing, and *k* is a slack/correction factor).
2. String-to-String (L_{str}): The parallel interconnection wiring.
3. Array-to-Inverter (L_{inv}): The main DC feeder run (Home-run).

Equation (9) gives the resulting power loss (P_{loss}) which is directly proportional to the total resistance (R_{total}).

$$P_{loss} = I^2 * R_{total} \quad (9)$$

2.15 Analytical Derivation of Quadratic Loss in Parallel Busbars

A critical design challenge in residential PV is the placement of the DC combiner bus. As the distance between the array and inverter increases, the "Main DC Bus" (the shared conductor) becomes the dominant source of system inefficiency.

2.15.1 The Quadratic Growth Principle

Equation (10) gives the energy dissipated as heat in the parallel bus (P_{bus}), derived from the aggregate current of all strings.

$$P_{bus} = (N_s * I_{str})^2 * (r * L_{bus} * C) \quad (10)$$

N_s: Number of parallel strings, I_{str}: Current per string (A), r: Resistance per meter (Ω/m) of the bus conductor, L_{bus}: Length of the shared us path (m)
C: Geometric layout factor accounting for non-uniform current distribution.
Critical Analysis: Equation 11 demonstrates that $P_{bus} \propto N_s$. Doubling the number of strings does not merely double the losses; it quadruples the power dissipation within the shared bus. This quadratic relationship necessitates sub-array partitioning in larger residential systems to maintain efficiency.

2.15.2 Simulation Analysis: String Scaling vs. Efficiency

To visualize this effect, a Python simulation was conducted comparing a single-block array against a partitioned sub-array.

Table 3: Simulated Power Loss Comparison

Number of Strings (Ns)	Total Current (A)	Theoretical Loss (W)	Partitioned Loss (W)
2	18.0	12.4	12.4
4	36.0	49.6	28.2
6	54.0	111.6	52.8

The results in Table 3 (plotted in Fig 2.2) confirm that as N_s increases, the "Power Loss Penalty" grows exponentially. This validates the study's recommendation for utilizing localized combiner boxes (Fig 2.3) to transition to high-voltage, low-current DC transmission as early as possible in the wiring topology.

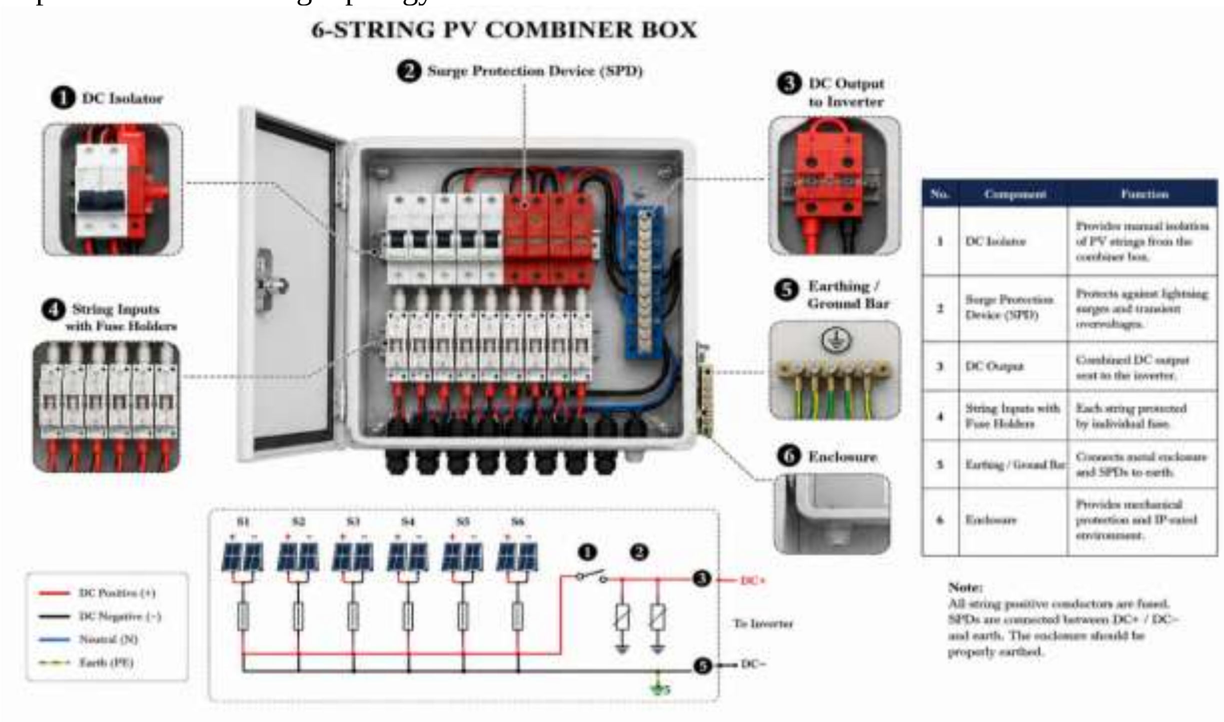

Fig 2.3: Integrated Combiner Box with Overcurrent Protection.

The use of a combiner box (as shown above) allows for the consolidation of strings into a single high-capacity feeder, but the methodology emphasizes that this "Bus" segment must be kept as short as possible to mitigate the N_s loss factor identified in our modelling.

2.16 Analysis of Blocking Diode Parasitic Losses and Thermal Impact

In parallel-connected PV architectures, blocking diodes are essential protective elements used to prevent the "Back-Feeding" phenomenon. When multiple strings are tied to a common DC bus, a voltage differential—caused by partial shading, localized soiling, or non-uniform degradation—can transform a low-performing string into a load rather than a generator.

2.16.1 The Physics of Reverse Current Prevention

Without blocking diodes, the string with the highest potential (V_{max}) drives a reverse current (I_{rev}) into shaded or mismatched strings (V_{low}), leading to:

1. Thermal Stress: Accelerated “Hot-spot” formation within individual cells.
2. Energy Cannibalization: The array consumes its own generated power, significantly lowing the aggregate Performance Ratio (PR).
3. MPPT Instability: The inverter’s Maximum Power Point Tracker may fail to find a global peak due to multiple local maxima created by string mismatch.

2.16.2 Mathematical Modelling of Power Dissipation

While blocking diodes provide safety, they introduce a permanent parasitic loss due to their internal barrier potential. The power dissipated as heat in a single diode (P_d) is modelled in equation (11).

$$P_d = V_f * I_{str} \quad (11)$$

V_f: Forward voltage drop (V), which is a function of the junction temperature and current.

I_{str}: String operating current (A)

For an array comprising *n* parallel strings, the cumulative power loss ($P_{d,total}$) is modelled in equation (12).

$$P_{d,total} = \sum_{i=1}^{n}(V_{f,i} * I_{str,i}) \quad (12)$$

2.16.3 Diode Selection Criteria and Efficiency Impact

The study evaluates the selection of diode technology based on the Forward Voltage (V_f) vs. Efficiency trade-off. Standard Silicon (Si) diodes typically exhibit a V_f of 0.7V, whereas Schottky Barrier Diodes are preferred in residential PV for their lower V_f (typically at operating temperatures).

Table 4: Comparative Efficiency Impact of Diode Technology

Diode Type	V_f $(at\ 25 \circ C)$	V_f (at 75∘C)	Est. Power Loss (per 10A String)
Standard Silicon	!.0 V	0.85 V	8.5 - 10.0 W
Schottky Barrier	0.55 V	0.42 V	4.2 - 5.5 W

2.16.4 Thermal Implications and Degradation

A critical finding in this analysis is the Inverse Thermal Relationship: as the ambient temperature in tropical regions increases, (V_f) slightly decreases, marginally reducing power loss. however, excessive heat leads to increased Reverse Leakage Current, which can degrade the diode's blocking capability over time.

Therefore, the methodology specifies that blocking diodes must be rated for at least $2 * V_{oc}$ of the string and housed in ventilated combiner boxes to prevent thermal runaway, as the heat dissipated P_d contributes to the localized temperature rise within the BOS enclosures.

3. Results and Discussion

3.1 Effect of Temperature and Solar Irradiance on PV Output

Fig 3.1 shows the simulated variation of normalised PV module power as a function of cell temperature for different irradiance levels (400–1000 W/m²). As expected, increasing irradiance increases the available output power at a given temperature, while increasing cell temperature causes a monotonic reduction in power across all irradiance levels. This behaviour is consistent with the analytical PV model, where higher irradiance primarily increases short-circuit current, whereas higher temperature narrows the semiconductor band gap, increasing dark saturation current and reducing open-circuit voltage.

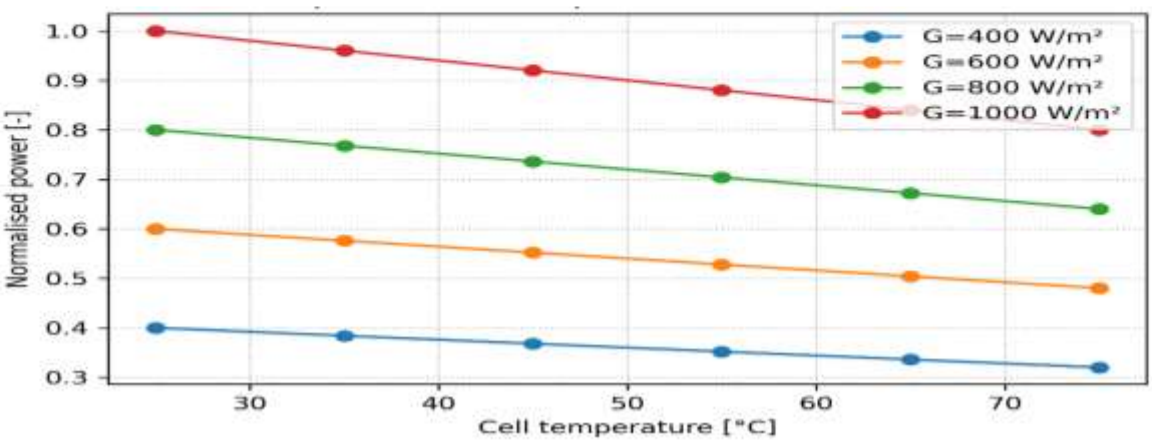

Fig 3.1: Effect of temperature on PV power at different irradiance levels

3.1.2 Statistical Summary

Table 3.1: Statistical Summary

	G = 400 W/m²	G = 600 W/m²	G = 800 W/m²	G = 1000 W/m²
Mean power	0.362	0.542	0.722	0.900
Total reduction	0.08	0.12	0.155	0.20
Percentage reduction	20%	20%	19.4%	20%

3.1.3 Temperature Coefficient

For the highest irradiance:

$$\Delta P = 1.00 - 0.80 = 0.20$$

Temperature increase:

$$75 - 25 = 50^oC$$

Power reduction rate:

$$\frac{0.20}{50} = 0.004$$

Thus, this is close to the typical temperature coefficient of commercial silicon PV modules.

3.1.4 Key Findings

1. Power decreases approximately linearly with increasing cell temperature.
2. An increase in cell temperature causes power loss.
3. Higher irradiance produces more power, but the temperature-related reduction remains proportional.
4. At 1000 W/m², power drops from 100% to 80% as temperature rises from 25°C to 75°C.

3.2 Environmental Factors: Dust Accumulation and Maintenance Intervals

Fig 3.2 presents an idealised model in which relative daily energy decreases approximately linearly by 3% per week without cleaning, up to eight weeks. Although the exact rate of soiling loss depends on local conditions, the trend is representative of many dry, dusty environments. After six to eight weeks without cleaning, the model predicts a reduction in daily energy to about 70–80% of the clean-panel value, consistent with reported field measurements in arid regions.

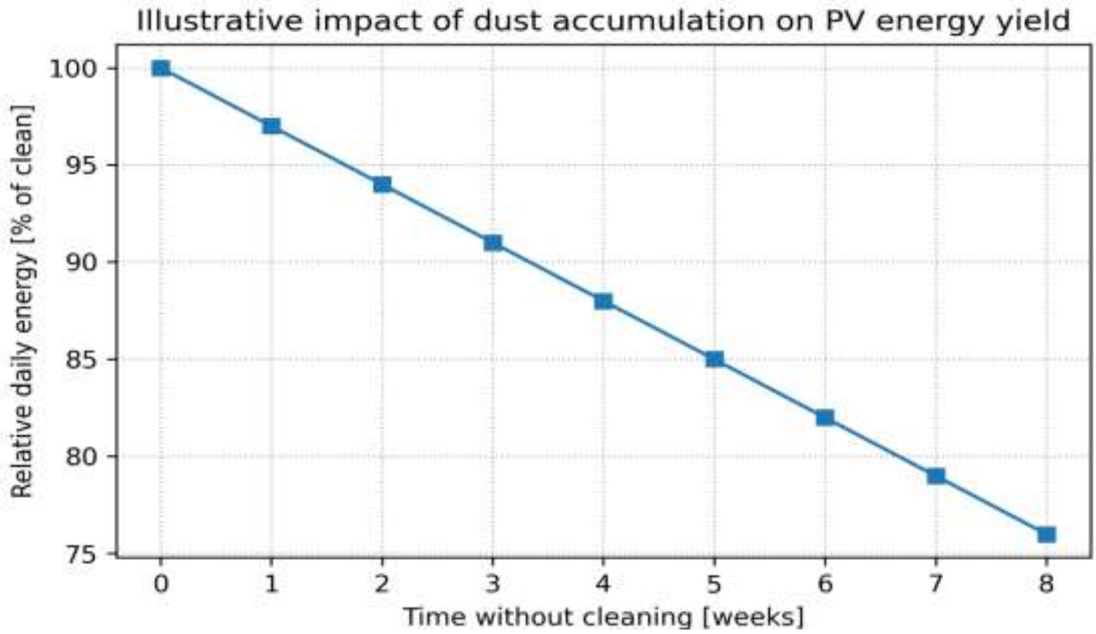

Fig 3.2: Illustrative impact of dust accumulation on PV energy yield

3.2.1 Statistical Summary

1. Maximum yield = 100%
2. Minimum yield = 76%
3. Mean yield = 88%
4. Median yield = 88%
5. Range = 24 percentage points

3.2.2 Key Findings

1. Energy yield declines almost perfectly linearly with dust accumulation.
2. Every week without cleaning reduces output by approximately 3%.
3. After weeks of increase dust collection on panels, output drops.
4. Regular cleaning can recover approximately 24% of lost energy production.

4. Conclusion

This study shows that real-world PV performance depends as much on environmental conditions and DC wiring practice as on the nominal module efficiency, and it integrates these aspects into a single engineering framework. The simulations confirm that increasing irradiance raises current and power while elevated cell temperature reduces open-circuit voltage and efficiency. Environmental stressors such as dust and wind reduce effective irradiance and humidity accelerates corrosion. Dust accumulation can cause multi-percent optical losses and non-uniform shading if cleaning is neglected, especially in dusty or coastal regions, which makes tailored cleaning schedules, appropriate tilt angles and robust enclosure sealing essential for sustained yield. The DC cabling analysis further demonstrates that poor conductor sizing and long runs can introduce voltage drops of several percent and additional I^2R losses, directly reducing energy delivered to the inverter; comparing calculated drops with the common 2% DC design guideline illustrates how appropriate conductor cross-section, route length and layout keep inverters within their MPPT windows. Taken together, these findings imply that field performance can be significantly improved not only by selecting efficient modules but also by intentionally managing temperature, soiling, humidity exposure and cabling, and they suggest that design rules such as fixed percentage voltage-drop limits should be refined with explicit consideration of climate and system topology.

References

1 P. Ollas, T. Thiringer, M. Persson, and C. Markusson, “Energy Loss Savings Using Direct Current Distribution in a Residential Building with Solar Photovoltaic and Battery Storage,” *Energies*, vol. 16, no. 3, p. 1131, Jan. 2023, doi: 10.3390/en16031131.

2 D. O. Johnson, K. A. Hassan, S. O. Okusanya, and J. O. Oladapo, “Solar Electricity System Design for Administrative Buildings,” *FUOYE J. Eng. Technol.*, vol. 5, no. 1, Mar. 2020, doi: 10.46792/fuoyejet.v5i1.458.

3 F. Schmid and F. Behrendt, “Optimal sizing of Solar Home Systems: Charge controller technology and its influence on system design,” *Sustain. Energy Technol. Assess.*, vol. 45, p. 101198, Jun. 2021, doi: 10.1016/j.seta.2021.101198.

4 T. Haruna, A. Ndem Ikot, and A. Big-Alabo, “A Review of Factors Affecting the Efficiency and Output of PV Systems Applied in the Tropical Climate of South-South Nigeria,” *Afr. J. Adv. Sci. Technol. Res.*, vol. 16, no. 1, pp. 01–17, Aug. 2024, doi: 10.62154/ajastr.2024.016.010328.

5 O. Bamisile, C. Acen, D. Cai, Q. Huang, and I. Staffell, “The environmental factors affecting solar photovoltaic output,” *Renew. Sustain. Energy Rev.*, vol. 208, p. 115073, Feb. 2025, doi: 10.1016/j.rser.2024.115073.

6 F. M. Oleiwi, J. S. Hameed, and Jaber. O. D. Dahloos, “Design and Feasibility Study of A Stand-Alone Home Pv Solar System in Baghdad Climate,” *Iraqi J. Sci.*, pp. 160–174, Jan. 2024, doi: 10.24996/ijs.2024.65.1.15.

7 E. H. Sepúlveda-Oviedo, “Impact of environmental factors on photovoltaic system performance degradation,” *Energy Strategy Rev.*, vol. 59, p. 101682, May 2025, doi: 10.1016/j.esr.2025.101682.

8 T. A. Dawood, R. R. I. Barwari, and A. Akroot, "Solar Energy and Factors Affecting the Efficiency and Performance of Panels in Erbil/Kurdistan," *Int. J. Heat Technol.*, vol. 41, no. 2, pp. 304–312, Apr. 2023, doi: 10.18280/ijht.410203.

9 W. S. Ebhota and P. Tabakov, "Influence of Cabling on Photovoltaic System Performance: Wire Length, Diameter, and Material," *Kurd. J. Appl. Res.*, vol. 10, no. 1, pp. 50–65, Mar. 2025, doi: 10.24017/science.2025.1.4.

10 A. Akšamović, S. Konjicija, S. Odžak, S. Pašalić, and S. Grebović, "DC Cabling of Large-Scale Photovoltaic Power Plants," *Appl. Sci.*, vol. 12, no. 9, p. 4500, Apr. 2022, doi: 10.3390/app12094500.

11 O. C. Chukwunedum, C. P. Nwachukwu, and C. O. Umobi, "Impact of solar PV power cable length on transmission efficiency in multi-building facility: Examining power loss in long-distance cable setups," 2025.

12 Eluan Oliveira Nascimento, Paulo Roberto Duailibe Monteiro, and Thiago Trezza Borges, "OPTIMIZATION OF CABLES IN A SOLAR POWER PLANT USING GENETIC ALGORITHMS," *Pap. Publ. Int. J. Adv. Eng. Technol. IJAET*, vol. Volume 16 Issue 6, p. December 2023. Available online at: https://www.ijaet.org/media/11I78IJAET1606318_v16_i6_pp608, Dec. 2023, doi: 10.5281/ZENODO.10518072.

13 C. Melios, A. Dimitriou, V. P. Androvitsaneas, I. F. Gonos, and C. A. Charalambous, "Determining the Insulation Resistance of DC Cables Used in Photovoltaic Systems Under Operational Conditions," *IEEE Trans. Ind. Appl.*, vol. 58, no. 6, pp. 6931–6941, Nov. 2022, doi: 10.1109/TIA.2022.3192736.

14 S. Czapp, S. Szultka, and A. Tomaszewski, "Design of Power Cable Lines Partially Exposed to Direct Solar Radiation—Special Aspects," *Energies*, vol. 13, no. 10, p. 2650, May 2020, doi: 10.3390/en13102650.

15 S. Czapp, S. Szultka, F. Ratkowski, and A. Tomaszewski, "Risk of power cables insulation failure due to the thermal effect of solar radiation," *Eksploat. Niezawodn. – Maint. Reliab.*, vol. 22, no. 2, pp. 232–240, Jun. 2020, doi: 10.17531/ein.2020.2.6.

16 T. Haruna, A. Ndem Ikot, and A. Big-Alabo, "A Review of Factors Affecting the Efficiency and Output of PV Systems Applied in the Tropical Climate of South-South Nigeria," *Afr. J. Adv. Sci. Technol. Res.*, vol. 16, no. 1, pp. 01–17, Aug. 2024, doi: 10.62154/ajastr.2024.016.010328.